Experimental Investigation of the Transformation Texture in Hot-Rolled Ferritic Stainless Steel Using Single Orientation Determination

D. RAABE and M. YLITALO

Two ferritic stainless steels (≈16.5 mass pct Cr) were hot-rolled using seven subsequent passes. The first sample was rolled within the range 1280 °C to 750 °C, *i.e.*, the deformation started in the ferritic region. The second sample was rolled within the range 1080 °C to 770 °C, *i.e.*, the deformation started in the ferritic-austenitic region. In both cases, up to 40 vol pct of the ferrite transformed into austenite during hot rolling. During the last passes, the austenite transformed into cubic martensite. After hot rolling, these former austenitic regions were identified using a selective etching technique and examined using single orientation determination in the scanning electron microscope. The regions which remained ferritic throughout the hot-rolling process were investigated as well. Whereas the texture of the martensite considerably depended on the hot-rolling conditions, especially on the temperature and on the intervals between the rollings, the texture of the ferrite was less affected. The textures of the martensite were interpreted in terms of the crystallographic transformation rules between austenite and martensite. The textures of the ferrite were discussed in terms of recovery and recrystallization.

I. INTRODUCTION

FERRITIC stainless steels containing 16 to 17 mass pct chromium and about 0.05 mass pct carbon represent an important group of high grade steels owing to their good corrosion resistance, high strength, and sufficiently good ductility. In some technical domains, *e.g.*, in the chemical, household, and automotive industry, ferritic stainless steels increasingly gain importance, since they can to a certain extent compete even with the expensive austenitic stainless steels.

The distribution of the crystallographic grain orientations of rolled and annealed ferritic stainless steels, which is hereafter referred to as texture, has been the subject of numerous studies in the past using the etch-pitting technique,[1] two-dimensional (2-D) centrosymmetric pole figures,[2] or the three-dimensional orientation distribution function (ODF).[3–6] The determination of the texture of ferritic stainless steels is of great importance for two reasons.

(1) The ODF represents an important weighting function of numerous macroscopical directional properties of a polycrystalline aggregate. In this context, especially the plastic properties, *e.g.*, the deep drawing behavior, more precisely the so-called ridging phenomenon, and the determination of the Lankfort value are of relevance. The ridging phenomenon, which is sometimes referred to as roping, is a surface defect which is developed during large strain deep drawing processes. This surface defect, which was identified by various authors to depend on the texture of the steel,[1–4,7,8] occurs parallel to the rolling direction and appears as narrow raised areas, similar to corrugations.

(2) The development of the texture during the various production steps is often determined by the physical processes involved in a rigorous crystallographic manner. Consequently, its determination provides a useful diagnostic probe for identifying the underlying metallurgical mechanisms of the main processing steps. In this context, the most important goals are the examination of crystallographic slip by correlating rolling textures with Taylor-type simulations,[3–5,9,10] of phase transformation by interpreting annealing and hot-rolling textures in terms of transformation rules and variant selection models,[11] and of recrystallization by correlating annealing textures with approaches based on growth selection,[12] preferred nucleation at grain boundaries,[13] and recovery.[10,14]

This investigation is concerned with the influence of the hot-rolling procedure on the texture of two ferritic stainless steels with about 16.5 mass pct Cr content which reveal up to 40 vol pct phase transformation during hot rolling. For the first time, the textures of both the transformed and the nontransformed regions were individually investigated employing a selective etching technique combined with single orientation determination in the scanning electron microscope. The results were compared to textures obtained by X-ray diffraction.

II. EXPERIMENTAL PROCEDURE

A. *Processing of the Specimens*

Two ferritic stainless steels with about 16.5 mass pct Cr and 0.05 mass pct C were hot-rolled using seven subsequent rolling passes. As is evident from Table I, the composition of both steels was nearly identical. The first specimen, HRC (HRC = hot-rolled, controlled), was rolled

D. RAABE, Group Head, is with the Institute for Physical Metallurgy and Metal Physics, Department of Materials Science, Kopernikusstr. 14, 52056 Aachen, Germany. M. YLITALO, formerly with the Department of Mechanical Engineering, University of Oulu, 90570 Oulu, Finland, is Research Fellow, Institute for Physical Metallurgy and Metal Physics.

Manuscript submitted April 3, 1995.

Table I. Chemical Composition of the Investigated Ferritic Stainless Steels in Mass Percent

Specimen	Cr	C	Si	Mn	Ni	N	Maximum Austenite
HRC (controlled)	16.3	0.05	0.27	0.52	0.1	0.04	43 vol pct
HRS (standard)	16.5	0.05	0.29	0.47	0.1	0.04	37 vol pct

in the temperature range 1280 °C to 750 °C, and the second specimen, HRS (HRS = hot rolled, standard), was rolled in the range 1080 °C to 770 °C (Table II). For both samples, the upper transformation temperature which separates the single-phase field of the high-temperature ferrite from the two-phase field in which both ferrite and austenite are stable amounts to 1250 °C (A5). Figure 1 shows that the transition to the low-temperature ferrite takes place at 880 °C (A1). Hot rolling of the specimen HRC started in the ferrite single-phase field, while hot rolling of the specimen HRS started in the ferrite-austenite two-phase field. The rolling schedules are given in Table II. In both cases, about 40 vol pct of the ferrite transformed to austenite during hot rolling. Table III shows the intervals between the rollings for sample HRC. It may be assumed that in the interval between pass 1 and pass 2 (45 seconds), the formation of the austenite was nearly completed. In the case of specimen HRS, the intervals between the rolling passes amounted to less than 5 seconds and may thus be neglected. During cooling, the austenite transformed to cubic martensite[15] (Table II). After hot rolling, both samples were box-annealed at 850 °C for 6 minutes. Since the transformed austenite was easily identified in the etched micrographs, it is obvious that this final annealing treatment did not suffice for achieving complete transformation of the martensite into ferrite. Hence, in the following, this phase will be referred to as relaxed or cubic martensite.

B. *Microstructure*

The microstructure was investigated after grinding, electropolishing, and final etching. For electropolishing, a solution of 78 mL $HClO_4$, 120 mL H_2O, 700 mL ethanol, and 100 mL $C_6H_{14}O_2$ was used, and for conventional metallography, a solution of 15 mL HNO_3, 30 mL HCl, and 45 mL glycerol was used. For the selective etching, which was employed to differentiate between the stable ferrite and the cubic martensite after hot rolling, a boiling solution of 200 mL H_2O, 60 mL HCl, and 5 g $FeCl_3$ was employed. In Figure 2, the dark-etching bands are relaxed martensite (former austenite) and the bright-etching areas are stable ferrite, which did not undergo phase transformation during hot rolling.

C. *Texture Measurement and ODF Calculation*

The crystal textures of the hot-rolled and annealed specimens were examined employing both statistical and local orientation determination. In the first case, the four pole figures {110}, {200}, {112}, and {103} were measured in the back reflection mode[16] within the range of the pole distance angle α from 5 to 85 deg using $Mo_{K\alpha}$ radiation. In order to remove a layer of $20 \cdot 10^{-6}$ m, the specimens were etched in a solution of 50 mL H_2O_2 and 10 mL HF prior to measurement. From the 2-D, centrosymmetric pole figures, the ODF was computed using the harmonic method ($l_{max} = 22$).[6] Using this technique provided quantitative orientation data stemming from both ferrite grains, which were not affected by phase transformation, and martensite grains, which were transformed from the austenite. Since the lattice parameters of both phases were identical in practical terms, the ODFs which were achieved from X-ray diffraction represented the overall texture of both phases. However, due to the missing spatial resolution, this technique did not allow differentiation between both types of phases. In the second case, the texture was examined in grain scale, exploiting the orientation dependence of electron backscattering diffraction (EBSD).[17] This technique represents a pertinent means of providing both microstructure and texture data with a high spatial resolution, which, together with the selective etching technique, allows differentiation between stable ferrite and relaxed cubic martensite. From the single orientation data, the ODF was computed by representing each grain by a Gauss function with a scatter width of 8 deg in Euler space.[18] Since we measured less than 1000 single orientations per ODF, we used this large value to artificially smooth the texture. Details of the EBSD technique employed were explained elsewhere.[19] All texture measurements were carried out in the center layer of the specimens.

D. *Presentation of Textures*

In case of cubic crystal symmetry and orthorhombic sample symmetry, an orientation can be presented by using the three Euler angles φ_1, ϕ, and φ_2 or the Miller indices $\{hkl\}\langle uvw\rangle$, where the first triple indicates the crystallographic plane parallel to the sheet surface and the second one the crystal vector parallel to the rolling direction. In this context, it should be mentioned that the hot-rolling process is not generally orthorhombic in symmetry. However, thorough finite element calculations on hot rolling of steel[20] have demonstrated that in the center layer of the sheet, ideal plain strain conditions prevail. This means that for interpreting the textures observed, orthorhombic conditions may be stipulated. Relevant texture components, which are typically generated during hot rolling of ferritic stainless steels,[3–5,21] are positioned on the so-called α fiber, γ fiber, and ε fiber. The α fiber at $\varphi_1 = 0$ deg and $\varphi_2 = 45$ deg comprises all texture components with a crystallographic $\langle 110\rangle$ direction parallel to the rolling direction. The γ fiber at $\phi = 54.7$ deg and $\varphi_2 = 45$ deg includes all texture components with a crystallographic $\langle 111\rangle$ direction parallel to the normal direction of the sheet. The ε fiber at $\varphi_1 = 90$ deg and $\varphi_2 = 45$ deg comprises all texture components with a crystallographic $\langle 110\rangle$ direction parallel to the transverse direction. Figure 3 shows some relevant texture components in Euler space.

III. EXPERIMENTAL RESULTS

A. *Microstructure*

Figure 2(a) shows that the microstructure of the sample HRC (longitudinal sections) contained ferritic grains (bright) with both equiaxed recrystallized and elongated re-

Table II. Hot-Rolling Schedules

Specimen	Heating*	Pass 1	Pass 2	Pass 3	Pass 4	Pass 5	Pass 6	Pass 7
HRC (controlled)	1280 °C	ε = 20 pct 1250 °C	ε = 30 pct 1080 °C	ε = 30 pct 1000 °C	ε = 35 pct 1000 °C	ε = 30 pct 950 °C	ε = 20 pct 800 °C	ε = 15 pct 750 °C
HRS (standard)	1080 °C	ε = 20 pct 1050 °C	ε = 35 pct 980 °C	ε = 35 pct 950 °C	ε = 30 pct 950 °C	ε = 32 pct 900 °C	ε = 25 pct 850 °C	ε = 17 pct 770 °C

*Prior to hot rolling the samples were annealed for 1 h. The temperatures given were taken after each pass.

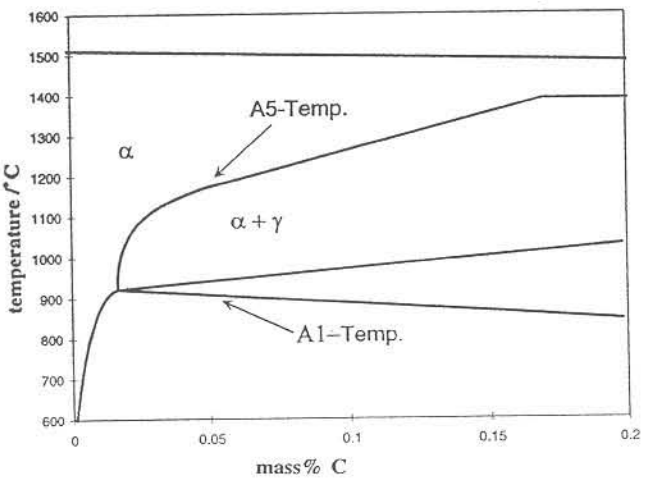

Fig. 1—Phase diagram showing the A5 temperature ($T_{A5} \approx 1250$ °C) and the A1 temperature ($T_{A1} \approx 880$ °C) of the alloys under investigation.

covered morphology. Additionally, flat elongated martensite grains appeared (dark). Figure 2(b) shows that the sample HRS contained mainly elongated ferritic grains (bright). Very small recrystallized grains were observed between the elongated martensitic regions (arrows). However, from these micrographs, it cannot be decided whether they were ferritic or martensitic prior to recrystallization.

B. *Texture*

Figure 4 shows the texture of the hot-rolled and annealed specimen HRC, and Figure 5 shows that of the specimen HRS. Figure 6 presents the corresponding fiber diagrams. Figure 4(a) shows the orientation distribution of the sample HRC in φ_1 sections through Euler space as determined by X-ray measurement. Since the lattice parameter of the cubic martensite is nearly identical to that of the stable ferrite, this ODF represents the texture of both phases. Figure 6(a) shows that the overall texture consists of an incomplete α fiber, ranging from $\varphi_2 = 0$ to $\approx$30 deg and a weak texture component close to $\{111\}\langle 112\rangle$. From Figure 6(c), it becomes apparent that the latter orientation is shifted by 10 deg about the transverse direction from its ideal position at $\phi = 54.7$ deg. Figure 4(b) presents the overall texture as determined on the basis of the single orientation measurements. Although both ODFs (Figures 4(a) and (b)) essentially reveal a strong resemblance, two deviations are obvious. The texture obtained from the local orientation determination is characterized, first, by a weaker and less homogeneously shaped incomplete α fiber and, second, by a stronger component close to $\{111\}\{112\}$ when compared to the X-ray texture. This deviation is attributed to the statistics of the EBSD measurements. After plotting the overall texture (Figure 4(b)), the single orientation data were decomposed according to the results of the selective etching technique into the ODF of the stable ferrite (Figure 4(c)) and the ODF of the cubic martensite (Figure 4(d)). According to these textures, the ferrite grains are mainly located on the incomplete α fiber between 10 and 60 deg, while the relaxed martensite grains reveal a main component close to $\{111\}\langle 112\rangle$ (Figure 6(b)) and minor components at $\{001\}\langle 110\rangle$ and $\{112\}\langle 110\rangle$ (Figure 6(a)).

Figure 5(a) shows the texture of both the cubic martensite and the ferrite in the specimen HRS as obtained from the X-ray experiments. The texture is similar to that of the corresponding specimen HRC (Figure 4(a)). However, the maximum occurring orientation density $f(g)_{max}$ exceeds that of the specimen HRC by a factor of 2 (Figures 6(a) and (c)). Figure 5(b) shows the texture of the relaxed martensitic and of the ferritic grains as determined from the single orientation data. Both ODFs (Figures 5(a) and (b)) show a good correspondence. However, the texture computed from the single orientation data reveals a stronger $\{112\}\langle 110\rangle$ and weaker $\{111\}\langle 112\rangle$ component as compared to the texture obtained from the X-ray measurements. Figure 5(c) shows the texture of the ferritic grains, and Figure 5(d) shows that of the relaxed martensitic grains. Whereas the ferrite reveals a dominant $\{001\}\langle 110\rangle$ texture component (Figures 5(c) and 6(a) and (c)), the relaxed martensite is characterized by a strong $\{112\}\langle 110\rangle$ orientation (Figures 5(d) and 6(a)).

IV. DISCUSSION

The X-ray textures of both types of specimens, HRC and HRS, which represent the orientation distribution of both the ferrite and the relaxed cubic martensite phase are quite similar (Figures 4(a) and 5(a)). Both ODFs reveal an incomplete α fiber and a weak $\{111\}\langle 112\rangle$ orientation. This observation is in good accord with previous investigations on various types of hot-rolled ferritic stainless steels.[3–5,22,23] However, in earlier studies, where steels with up to 40 vol pct phase transformation during hot rolling were studied, it was not possible to differentiate between the texture of the relaxed martensite and that of the ferrite. Hence, interpretations of the textures observed with respect to the influence of phase transformation often remained somewhat vague. Nevertheless, it seems likely that the orientation distribution of the nontransformed ferritic grains in the samples under investigation is similar to the texture of hot-rolled ferritic stainless steels with negligible phase transformation.[3,4,5]

Figures 4(c) and 5(c) show the single-phase textures of the ferrite. It becomes apparent that a major portion of the α fiber, which characterizes the overall textures (Figures 4(a) and 5(a)), indeed corresponds to the ferrite textures. This applies especially for the specimen HRS (Figures 5(a) and (c)), where the ferrite phase reveals a strong

Table III. Hot-Rolling Schedule of Sample HRC; Intervals between the Rolling Passes

Passes	Pass 1 ε = 20 pct	Pass 2 ε = 30 pct	Pass 3 ε = 30 pct	Pass 4 ε = 35 pct	Pass 5 ε = 30 pct	Pass 6 ε = 20 pct	Pass 7 ε = 15 pct
Intervals (s)	45	15	15	15	15	≈5	

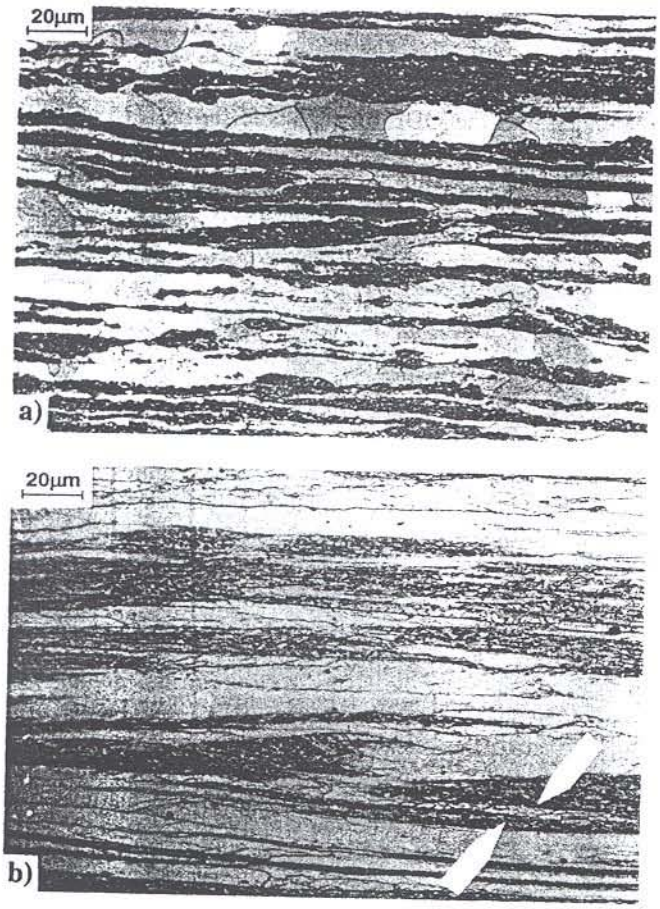

Fig. 2—Longitudinal micrographs, hot-rolled and annealed at 850 °C for 6 min. (*a*) Sample HRC showing both equiaxed recrystallized and elongated recovered ferritic grains (bright) and flat elongated relaxed martensite grains (dark). (*b*) Sample HRS showing mainly elongated ferritic grains (bright) and some very small recrystallized grains between the elongated martensitic regions (arrows). From these micrographs, it cannot be decided whether they were ferritic or martensitic prior to recrystallization.

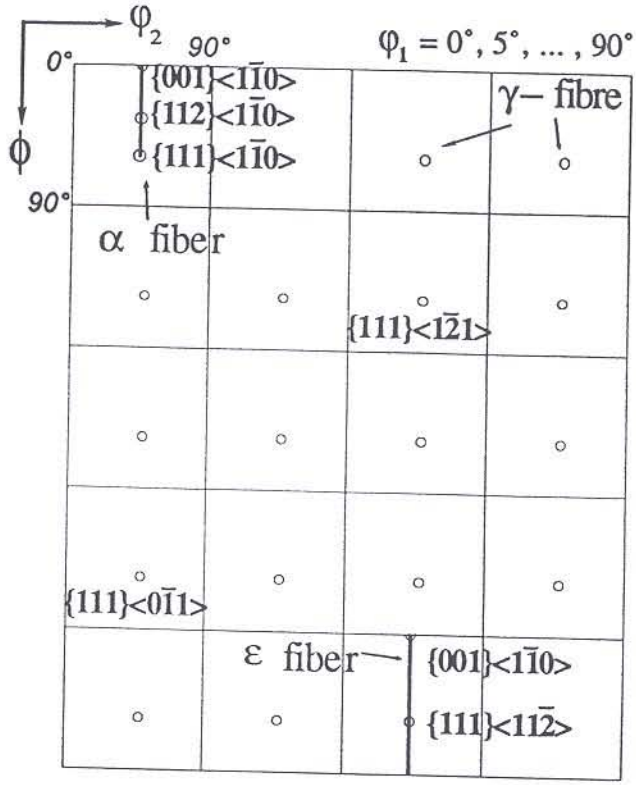

Fig. 3—Some relevant texture components of hot-rolled ferritic stainless steels given in φ_1 sections through Euler space.

{001}⟨110⟩ texture which is spread about the rolling direction. In the case of sample HRC (Figures 4(a) and (c)), this correspondence is less pronounced. Although in the latter sample the ferrite phase reveals a weak incomplete α fiber (Figures 4(c)), the {001}⟨110⟩ component does not appear. According to the micrograph (Figure 2(a)), which reveals a large volume fraction of equiaxed ferrite grains, it is assumed that the ferrite texture of the sample HRC (Figure 4(c)) may be interpreted in terms of partial recrystallization. This assumption is advocated by three facts. First, hot rolling of the sample HRC started at a very high temperature of 1280 °C. Since the kinetics of recrystallization of ferritic stainless steels is affected by the presence of carbides and solute atoms on grain boundaries, such an elevated hot-rolling temperature should promote recrystallization rather than recovery. Second, the ferrite texture (Figure 4(c)) reveals a pronounced {111}⟨110⟩ orientation, which is among the main recrystallization components of conventionally cold-rolled and annealed ferritic stainless steels.[24,25] Third, the intervals between the rolling passes (Table III), as used in the case of sample HRC, represent potential incubation periods, *i.e.*, they promote the formation of recrystallization nuclei.

In contrast, the strong {001}⟨110⟩ component observed in the sample HRS is attributed to recovery. In various investigations on cold-rolled and annealed ferritic stainless steels,[24,25] it was observed that upon annealing at low temperatures, recovery prevailed, while at high temperatures, recrystallization prevailed. Consequently, the relatively low temperature at the beginning of hot rolling of the sample HRS (1080 °C) advocates recovery. In contrast to the sample HRC, in the case of sample HRS, the intervals between the rolling passes were negligible, which deteriorates the nucleation conditions. Moreover, recovery is not only stimulated by the temperature range but also by the orientation of the grains affected. Numerous observations on pure iron,[26] low-carbon steels,[27,28,29] iron with 3 pct silicium,[30,31,32] and ferritic stainless steels[4,24,25] have substantiated that {001}⟨110⟩ oriented grains have a strong tendency to recovery rather than to recrystallize. Such behavior of {001}⟨110⟩ and {001}⟨100⟩ oriented grains was interpreted in terms of the dislocation cell and microband structures characteristic of such crystals and the resulting

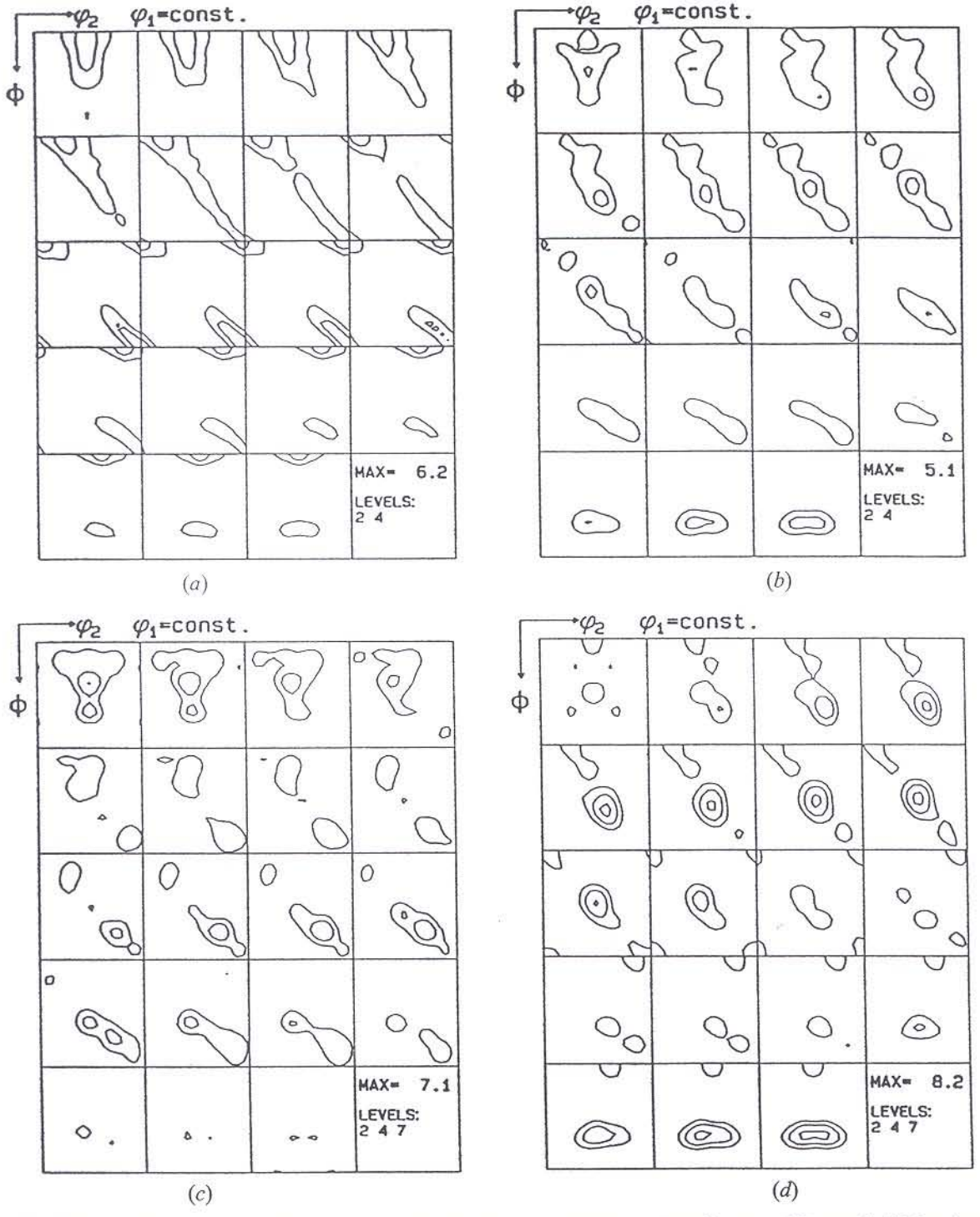

Fig. 4—Crystallographic texture of the hot-rolled and annealed specimen HRC in φ_1 sections. (*a*) Overall texture of the sample HRC as determined by the X-ray measurement. Since the lattice parameter of the relaxed martensite is nearly identical to that of the stable ferrite, this ODF contains the texture of both phases. (*b*) Overall texture of the sample HRC as determined by the single orientation measurements. The deviation to (a) is due to the statistics of the EBSD measurements. (*c*) Texture of the grains which remained ferritic throughout the hot-rolling process as determined by the single orientation measurements (bright areas in Fig. 2(a)). (*d*) Texture of the relaxed martensite phase as determined by the single orientation measurements (dark areas in Fig. 2(a)).

local orientation gradients which did not suffice to generate kinetic instabilities required for recrystallization. This interpretation of the ferrite texture of the sample HRS corresponds to the micrograph (Figure 2(b)), which shows elongated instead of equiaxed ferrite grains. Recrystallization was observed only in some narrow regions, which were surrounded by relaxed martensite. However, it cannot be excluded that these areas (arrows) were generated by the recrystallization of relaxed martensite.

The textures of the cubic martensite phase (Figures 4(d) and 5(d)) may be discussed in terms of the Nishiyama–Wassermann (NW)[33,34] transformation rules. According to NW, a {111} lattice plane and a ⟨112⟩ lattice vector in the austenite correspond to a {110} plane and a ⟨110⟩ vector

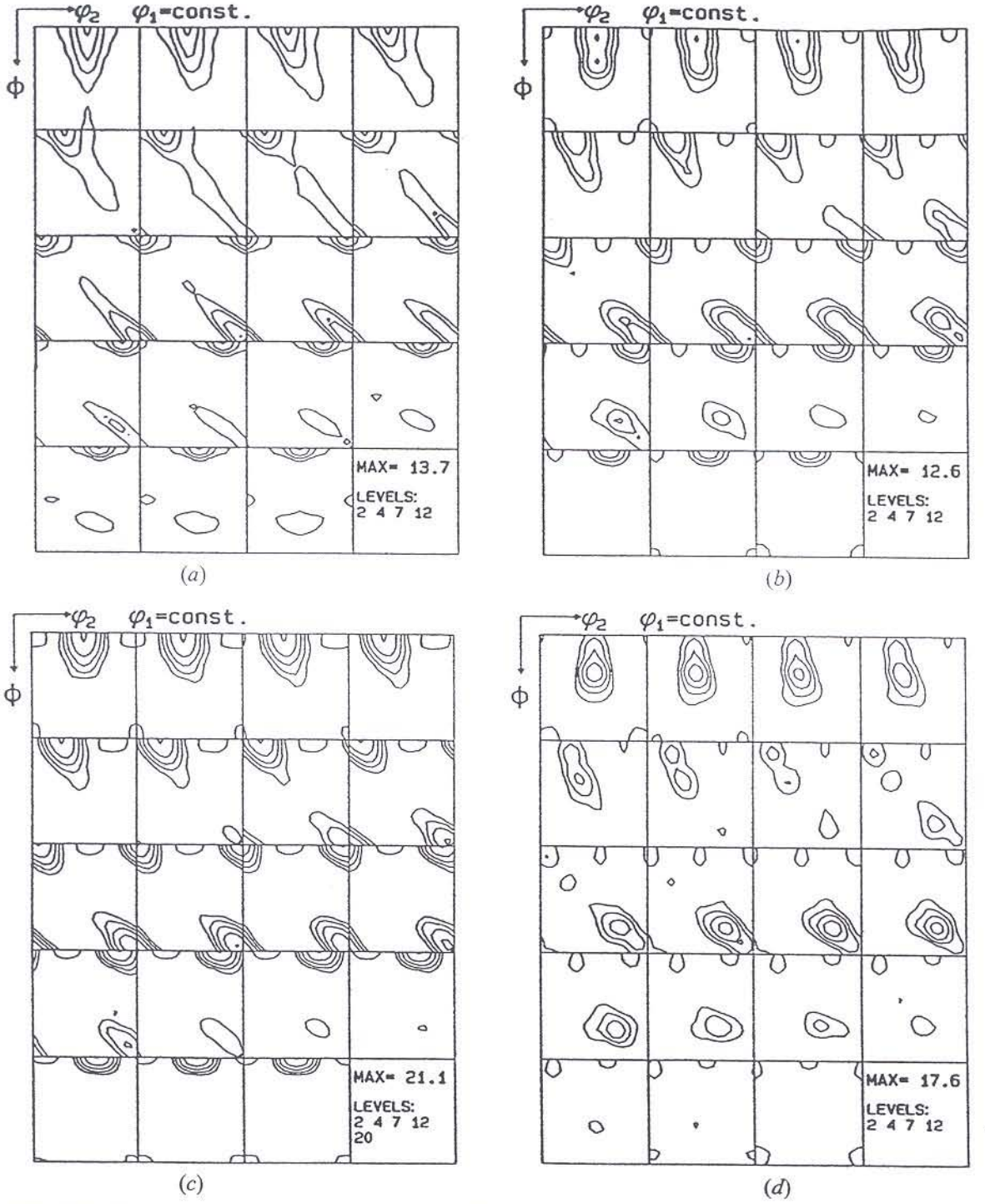

Fig. 5—Crystallographic texture of the hot-rolled and annealed specimen HRS in φ_1 sections. (*a*) Overall texture of the sample HRS as determined by the X-ray measurement. Since the lattice parameter of the relaxed martensite is nearly identical to that of the stable ferrite, this ODF contains the texture of both phases. (*b*) Overall texture of the sample HRS as determined by the single orientation measurements. The deviation to (a) is due to the statistics of the EBSD measurements. (*c*) Texture of the grains which remained ferritic throughout the hot-rolling process as determined by the single orientation measurements (bright areas in Fig. 2(b)). (*d*) Texture of the relaxed martensite phase as determined by the single orientation measurements (dark areas in Fig. 2(b)).

in the relaxed martensite. Following Davies *et al.*,[35] these transformation rules can be expressed in terms of a 95.3 deg rotation about a common $\langle hkl \rangle$ axis with $h = -1 + \sqrt{2} + \sqrt{3}$, $k = 1 + \sqrt{2} + \sqrt{3}$, and $1 = \sqrt{2}$. The prediction of the textures of body centered cubic product phases from a given face centered cubic (fcc) parent phase has been the subject of various thorough studies in the past using pole figures[36] or ODFs.[11,35]

In the present work, the transformation rules must be used inversely, since the texture of the austenite must be deduced from the experimentally achieved texture of the cubic martensite. Whereas the martensite texture in the

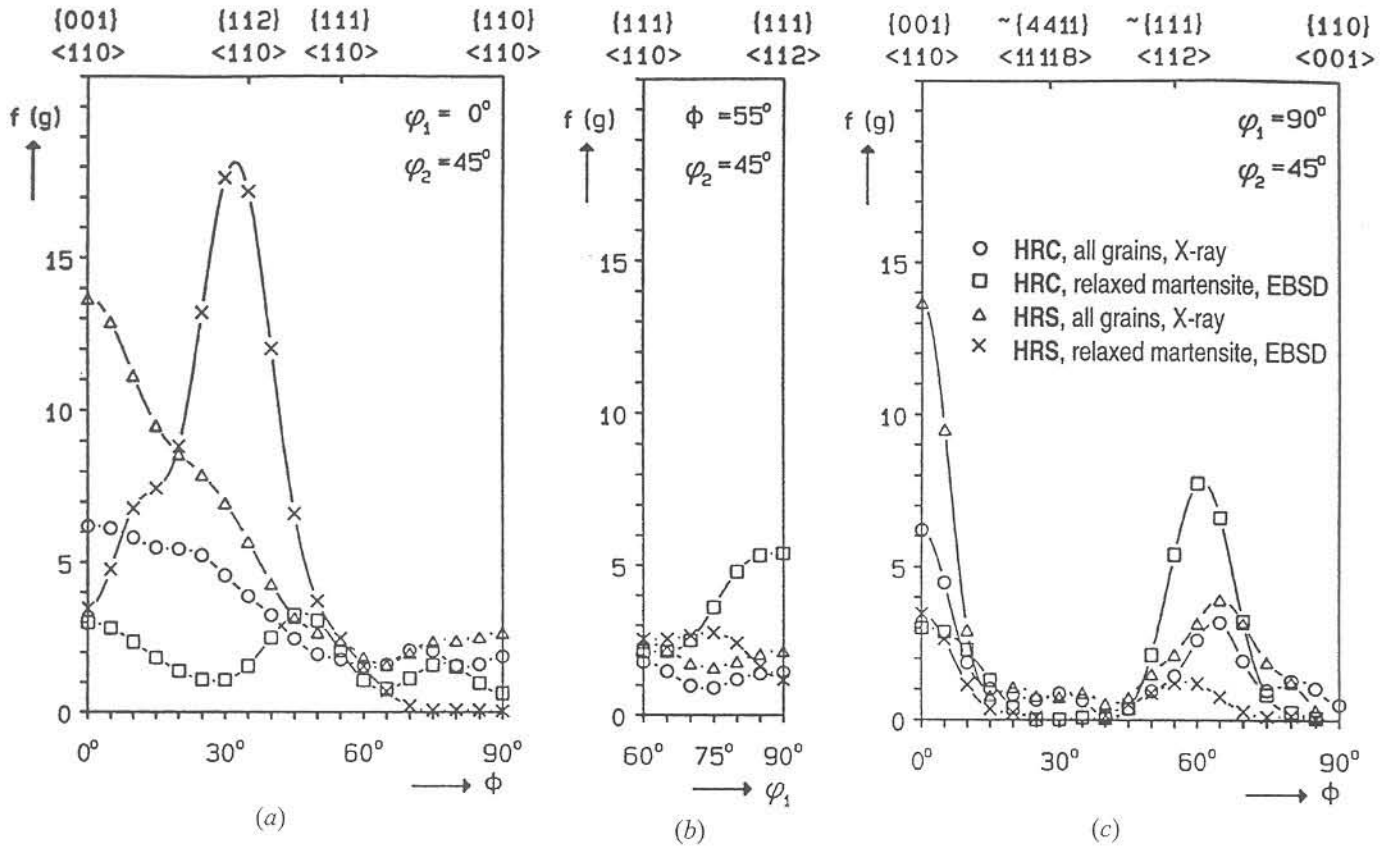

Fig. 6—Crystallographic texture of the hot-rolled and annealed specimens HRC and HRS in fiber presentation showing the overall textures as determined by the X-ray measurement and the texture of the relaxed martensite as determined by the single orientation measurements. The legend given in the right box applies to all three fiber diagrams: (*a*) α fiber, (*b*) γ fiber, and (*c*) ε fiber.

sample HRC (Figure 4(d)) was characterized by a strong component close to {111}⟨112⟩, the corresponding texture in the sample HRS revealed a dominant component close to {112}⟨110⟩ (Figure 5(d)). Earlier studies on transformation[11,35,36] suggested that in the context of hot rolling, variant selection seems to play a minor role. Therefore, a simple NW transformation of the experimentally observed ~{111}⟨112⟩ martensite component (Figures 4(d) and 6(c)) suggests an initial ~{110}⟨112⟩ orientation of the parent phase in the sample HRC. This texture component is well known from heavily cold-rolled austenitic stainless steels[37-39] and 70/30 brass.[40] In these alloys, the {110}⟨112⟩ orientation typically prevails after large degrees of deformation. Applying the NW rotation to the main martensite texture component of the sample HRS, ~{112}⟨110⟩ (Figure 5(d)), predicts an initial ~{112}⟨111⟩ orientation of the austenitic parent phase. This orientation prevails together with {110}⟨112⟩ in weakly cold-rolled austenite[37-39] and brass.[40] It is likely that the main texture components which develop during cold rolling of fcc alloys with a low stacking fault energy are also typical of the austenitic high-temperature phase of hot-rolled ferritic stainless steel. However, for obtaining a more detailed image of the stable orientations at elevated temperatures, the center layer texture of a hot-rolled stable austenitic stainless steel with 18 mass pct Cr and 10 mass pct Ni was additionally examined. As is evident from Figure 7, in the hot band texture, indeed the {112}⟨111⟩, {123}⟨634⟩, and especially {110}⟨112⟩ rolling components occurred, as did a weak {001}⟨100⟩ recrystallization component.

Transforming the martensite textures observed thus suggests that the austenitic phase during hot rolling was dominated by a strong {110}⟨112⟩ orientation in the case of specimen HRC and by a strong {112}⟨111⟩ orientation in the case of specimen HRS. Following the results stemming from comparable cold- and hot-rolled fcc alloys,[37,38,39,40] this means that the austenite in the sample HRS has undergone less deformation than the austenite in the sample HRC. However, such a conclusion seems to contradict the results obtained from the ferritic phase, which suggested strong deformation and recovery in the sample HRS and weak deformation and recrystallization in the sample HRC. This contradiction can be explained in terms of the strain, temperature, and time range where the austenite occurred during hot rolling and the recrystallization behavior of the austenite. Figure 1 and Table II show that hot rolling of the sample HRC started at 1280 °C, *i.e.*, in the high-temperature single-phase region of the ferrite. The maximum volume fraction of transformed austenite (~40 vol pct) presumably occurred during the interval between the rolling pass 1 and pass 2 (Tables II and III). Below a temperature of 880 °C, the austenite was no longer stable. It is likely that in the strain and temperature regime where austenite occurred (pass 2 through pass 5), the deformation imposed did not suffice for recrystallization but only for recovery and thus for the generation of a pronounced {110}⟨112⟩

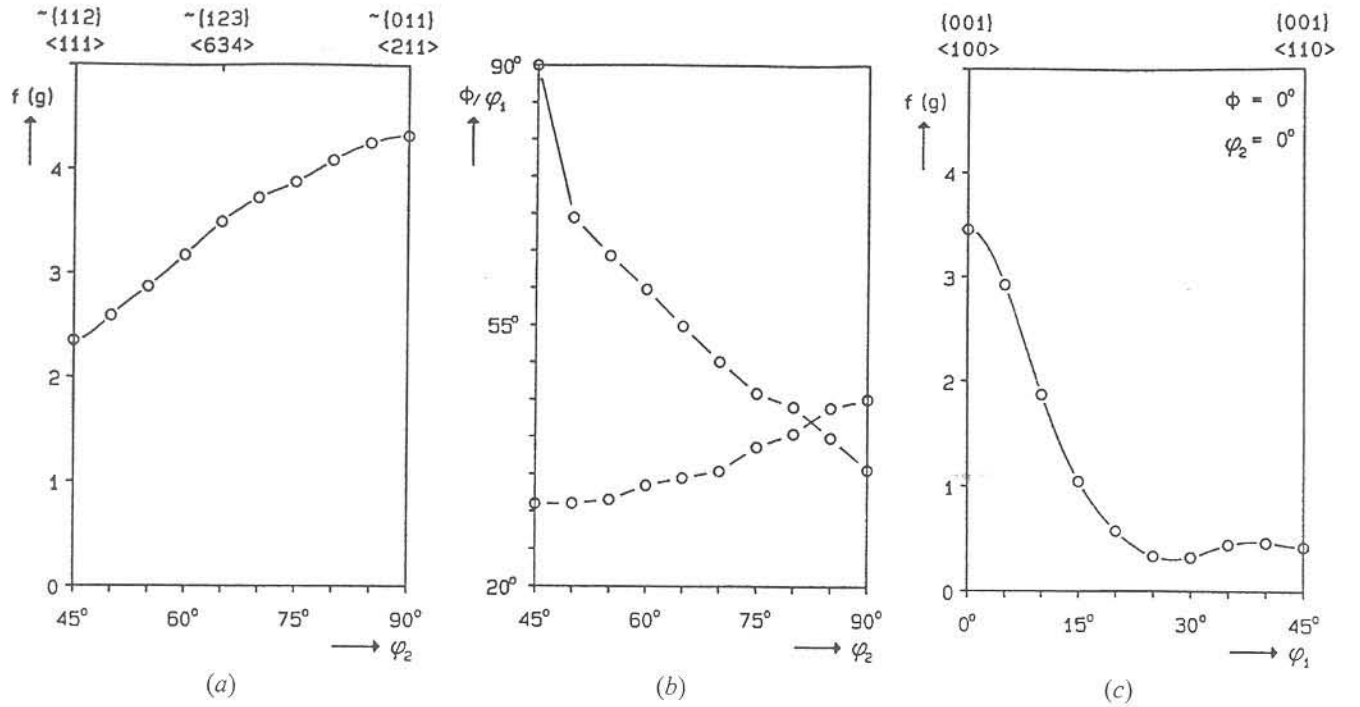

Fig. 7—Crystallographic texture in the center layer of a hot-rolled austenitic stainless steel with 18 mass pct Cr and 10 mass pct Ni as determined by X-ray measurement, fiber presentation: (*a*) β fiber (maximum density), (*b*) β fiber (coordinates in Euler space), and (*c*) cube rotation about the normal direction of the sheet.

rolling orientation. However, in the sample HRS, the first rolling pass was directly carried out in the two-phase region (Figure 1 and Table II) with a maximum volume fraction of transformed austenite. In the specimen HRS, the austenite remained stable down to pass 5 (Table II). This means the accumulated strain of the austenite in the sample HRS (pass 1 through pass 5) considerably exceeded that of the austenite in the sample HRC. It is thus concluded that the accumulated strain stimulated austenite recrystallization in the sample HRS during the first hot-rolling passes and the formation of a weak $\{112\}\langle 111\rangle$ texture component during the last rolling passes, which were carried out in the ferritic-austenitic two-phase region.

V. SUMMARY AND CONCLUSIONS

Two ferritic stainless steels with about 16.5 mass pct Cr content were hot-rolled and finally annealed. The first specimen was rolled in the temperature range 1280 °C to 750 °C, *i.e.*, deformation started in the ferritic region (sample HRC). The second sample was rolled within the range 1080 °C to 770 °C, *i.e.*, deformation started in the ferritic-austenitic region (sample HRS). In both cases, up to 40 vol pct of the ferrite transformed into austenite during hot rolling. Below 880 °C, the austenite transformed into cubic martensite. The transformed regions were identified by a selective etching technique. Both the relaxed martensite and the ferrite were examined employing single orientation measurements in the scanning electron microscope. The main results were as follows.

1. Whereas the texture of the relaxed martensite considerably depended on the hot-rolling conditions (different orientations, different orientation densities), the texture of the ferrite was less affected (similar orientations, different orientation densities).
2. The orientation distribution of the ferrite grains in both samples was characterized by an incomplete α fiber. The ferrite texture in the sample HRS was stronger than in the sample HRC. The differences were interpreted in terms of recovery in sample HRS (T_{start} = 1080 °C, no intervals between the rolling passes) and partial recrystallization in sample HRC (T_{start} = 1280 °C, intervals between the rolling passes).
3. The orientation distribution of the relaxed martensite grains in sample HRS was characterized by a $\sim\{112\}\langle 110\rangle$ component, which corresponds to a preceding $\sim\{112\}\langle 111\rangle$ orientation in the austenite. In the sample HRC, the relaxed martensite revealed a $\sim\{112\}\langle 112\rangle$ component, which corresponds to a preceding $\sim\{110\}\langle 112\rangle$ orientation. In the sample HRS, the austenite remained stable between pass 1 and pass 5. It was assumed that the accumulated strain stimulated austenite recrystallization during the first hot-rolling passes and the formation of a weak $\{112\}\langle 111\rangle$ component during the last rolling passes in the two-phase region. In the sample HRC, the austenite was stable presumably between pass 2 and pass 5. It was assumed that in this strain and temperature regime, deformation did not suffice for recrystallization but only for recovery and thus for the generation of a pronounced $\{110\}\langle 112\rangle$ rolling orientation.

ACKNOWLEDGMENTS

Financial support from the Foundation of Outokumpu Oy, the Academy of Finland, the Tauno Tönning Foundation, and the University of Oulu, as well as from Ou-

tokumpu Oy, is gratefully acknowledged by one of the authors (M.Y.).

REFERENCES

1. H.C. Chao: *Trans. ASM*, 1967, vol. 2, pp. 37-50.
2. R.M. Davison: *Metall. Trans. A*, 1975, vol. 6A, pp. 2243-48.
3. M. Hölscher, D. Raabe, and K. Lücke: *Steel Res.*, 1991, vol. 62, pp. 567-75.
4. D. Raabe and K. Lücke: *Mater. Sci. Technol.*, 1993, vol. 9, pp. 302-12.
5. M. Hölscher, D. Raabe, and K. Lücke: *Acta Metall.*, 1994, vol. 42, pp. 879-86.
6. H.J. Bunge: *Texture Analysis in Materials Science*, Butterworth and Co., London, 1982.
7. H.M. Kim and J.A. Szpunar: *Mater. Sci. Forum*, 1994, vols. 157–162, pp. 753-60.
8. K. Bethke, M. Hölscher, and K. Lücke: *Mater. Sci. Forum*, 1994, vols. 157–162, pp. 1137-44.
9. J.L. Raphanel and P. van Houtte: *Acta Metall.*, 1985, vol. 33, pp. 1481-88.
10. D. Raabe and K. Lücke: *Mater. Sci. Forum*, 1994, vols. 157–162, pp. 597-610.
11. R. Ray and J. Jonas: *Int. Mater. Rev.*, 1990, vol. 35, pp. 1-36.
12. G. Ibe and K. Lücke: *Arch. Eisenhüttenwes.*, 1968, vol. 39, pp. 693-704.
13. W.B. Hutchinson: *Acta Metall. Mater.*, 1994, vol. 37, pp. 1047-56.
14. D. Raabe: *Steel Res.*, 1995, vol. 66, pp. 222-29.
15. J.D. Defilippi and Hung-Chi Chao: *Metall. Trans.*, 1971, vol. 2, pp. 3209-16.
16. L.G. Schulz: *J. Appl. Phys.*, 20, 1949, pp. 1030-38.
17. J. Venables and C. Harland: *Phil. Mag.*, 27, 1973, pp. 1193-1200.
18. K. Lücke, J. Pospiech, K.H. Virnich, and J. Jura: *Acta Metall.*, 1981, vol. 29, pp. 167-85.
19. O. Engler and G. Gottstein: *Steel Res.*, 1992, vol. 63, pp. 413-18.
20. A.J. McLaren and C.M. Sellars: *Proc. Int. Conf. on Strip Casting*, Hot and Cold Working of Stainless Steels, City of Quebec, PQ, Canada, 1993, N.D. Ryan, A.J. Brown, and H.J. McQueen, eds., TMS-CIM, 1993, pp. 107-15.
21. D. Raabe and K. Lücke: *Scripta Metall.*, 1992, vol. 26, pp. 1221-26.
22. D. Raabe and K. Lücke: *Mater. Sci. Forum*, 1994, vols. 157–162, pp. 1469-74.
23. A. Fedosseev, D. Raabe, and G. Gottstein: *Mater. Sci. Forum*, 1994, vols. 157–162, pp. 1771-76.
24. D. Raabe and K. Lücke: *Mater. Sci. Forum*, 1994, vols. 157–162, pp. 1033-38.
25. D. Raabe and K. Lücke: *Steel Res.*, 1992, vol. 63, pp. 457-64.
26. D. Raabe and K. Lücke: *Scripta Metall.*, 1992, vol. 27, pp. 1533-38.
27. C. Smith and I.L. Dillamore: *Met. Sci.*, 1974, vol. 8, pp. 73-81.
28. I.L. Dillamore, P.L. Morris, C.J.E. Smith, and W.B. Hutchinson: *Proc. R. Soc.*, 1972, vol. 329A, pp. 405-12.
29. P. Swann and J. Nutting: *J. Inst. Met.*, 1961, vol. 90, pp. 133-42.
30. J. Walter and E. Koch: *Acta Metall.*, 1963, vol. 11, pp. 923-39.
31. H. Hu: *Trans. AIME*, 1962, vol. 224, pp. 75-88.
32. H. Hu: in *Recovery and Recrystallization of Metals*, L. Himmel, ed., John Wiley and Sons, New York, NY, 1963, pp. 311-78.
33. Z. Nishiyama: *Sci. Rep. Inst., Tohoku Univ.*, 1934–35, vol. 23, pp. 638-47.
34. G. Wassermann: *Arch. Eisenhüttenwes.*, 1933, vol. 16, pp. 647-58.
35. G.J. Davies, J.S. Kallend, and P.P. Morris: *Acta Metall.*, 1976, vol. 24, pp. 159-72.
36. A. Jones and B.R. Walker: *Met. Sci.*, 1974, vol. 8, pp. 394-405.
37. S.R. Goodman and H. Hu: *Trans. AIME*, 1964, vol. 230, pp. 1413-21.
38. C. Donadille, R. Valle, P. Dervin, and R. Penelle: *Acta Metall.*, 1989, vol. 37, pp. 1547-1571.
39. T.J. Rickert and J.A. Salsgiver: *Mater. Sci. Forum*, 1994, vols. 157–162, pp. 2017-24.
40. J. Hirsch, K. Lücke, and M. Hatherly: *Acta Metall.*, 1988, vol. 36, pp. 2863-2927.